

REPORT DOCUMENTATION PAGE

Form Approved
OMB No. 0704-0188

The public reporting burden for this collection of information is estimated to average 1 hour per response, including the time for reviewing instructions, searching existing data sources, gathering and maintaining the data needed, and completing and reviewing the collection of information. Send comments regarding this burden estimate or any other aspect of this collection of information, including suggestions for reducing the burden, to the Department of Defense, Executive Service Directorate (0704-0188). Respondents should be aware that notwithstanding any other provision of law, no person shall be subject to any penalty for failing to comply with a collection of information if it does not display a currently valid OMB control number.

PLEASE DO NOT RETURN YOUR FORM TO THE ABOVE ORGANIZATION.

1. REPORT DATE (DD-MM-YYYY) 1Apr 07		2. REPORT TYPE Final Report		3. DATES COVERED (From - To) 1 Apr 07 - 30 Nov 09	
4. TITLE AND SUBTITLE Shape Memory Alloys for Vibration Isolation and Damping of Large-Scale Space Structures				5a. CONTRACT NUMBER FA9550-07-1-0331	
				5b. GRANT NUMBER	
				5c. PROGRAM ELEMENT NUMBER	
6. AUTHOR(S) Dimitris C. Lagoudas, Tamás Kalmár-Nagy				5d. PROJECT NUMBER	
				5e. TASK NUMBER	
				5f. WORK UNIT NUMBER	
7. PERFORMING ORGANIZATION NAME(S) AND ADDRESS(ES) Texas A&M University College Station, TX 77843-3409				8. PERFORMING ORGANIZATION REPORT NUMBER	
9. SPONSORING/MONITORING AGENCY NAME(S) AND ADDRESS(ES) Air Force Office of Scientific Research 875 North Randolph Street Arlington, VA22203				10. SPONSOR/MONITOR'S ACRONYM(S) AFOSR/RSA	
				11. SPONSOR/MONITOR'S REPORT NUMBER(S) AFRL-AFOSR-VA-TR-2016-0685	
12. DISTRIBUTION/AVAILABILITY STATEMENT Distribution Statement A: Approved for public release. Distribution is unlimited.					
13. SUPPLEMENTARY NOTES					
14. ABSTRACT The US Air Force is currently pursuing large sparse aperture arrays with low-frequency structural design requirements to ensure that thermal and gravity gradient induced on-orbit disturbances do not excite the structure. Structures with these frequency response characteristics will need a larger error budget for active control due to their limitations to passively accommodate external excitations and meet their performance requirements. This work will investigate utilization of Shape Memory Alloys (SMAs) to enhance the passive structural stability of the structure, by taking advantage of the SMA capacity for large, recoverable deformations and hysteric response.					
15. SUBJECT TERMS Standard terms apply					
16. SECURITY CLASSIFICATION OF:			17. LIMITATION OF ABSTRACT UU	18. NUMBER OF PAGES	19a. NAME OF RESPONSIBLE PERSON Dimitris C. Lagoudas
a. REPORT U	b. ABSTRACT U	c. THIS PAGE U			19b. TELEPHONE NUMBER (Include area code)

Shape Memory Alloys for Vibration Isolation and Damping of Large-Scale Space Structures

AFOSR Grant: FA9550-07-1-0331

Dimitris C. Lagoudas, Tamás Kalmár-Nagy
Texas A&M University, College Station, TX 77843-3409, USA

Magdalini Z. Lagoudas
Spacecraft Technology Center, College Station, TX 77843-3118, USA

Supported Students

Luciano. G. Machado, Doctor of Philosophy 2007, Texas A&M University
Ashivni Shekhawat, Master of Science 2008, Texas A&M University
Bong Su Koh, Master of Science 2008, Texas A&M University

Undergraduate Research Assistants

Agustin F. Maqui, Texas A&M University (BS 2010)
Jack V. Heath, Texas A&M University (BS 2010)
Paul F. Braden, Texas A&M University (2011)

1 Introduction

The US Air Force is currently pursuing large sparse aperture arrays with low-frequency structural design requirements to ensure that thermal and gravity gradient induced on-orbit disturbances do not excite the structure. Structures with these frequency response characteristics will need a larger error budget for active control due to their limitations to passively accommodate external excitations and meet their performance requirements. This work will investigate utilization of Shape Memory Alloys (SMAs) to enhance the passive structural stability of the structure, by taking advantage of the SMA capacity for large, recoverable deformations and hysteretic response. SMAs can be pre-strained up to their transformation region and can act as constant force structural elements, in which loading variations will result in hysteretic damping due to phase transformation. Current use of SMAs as vibration isolation and damping devices is limited to small deformations and a constrained environment. Large space structures provide an opportunity to exploit the full potential of SMAs, while providing feasible technical solutions to a reliable design of such systems.

The main objectives of the project were to:

- 1) Develop a constitutive model for SMAs to properly describe thermomechanical coupling and to account for partial phase transformation under dynamic conditions; integrate the constitutive model into a finite element environment for design optimization of large space structures with SMA elements subjected to dynamical loadings.
- 2) Implement the model to analyze the dynamical response of a prototype passive vibration isolation and damping device, including investigations into complex oscillations.
- 3) Conduct an analytical and numerical investigation on the dynamics of a one-dimensional (1D) chain and a two-dimensional (2D) lattice of SMA oscillators, focusing on the influence of the use of SMA elements in vibration isolation and damping characteristics of these dynamical systems.
- 4) Investigate the stability of dynamical responses of near-periodic 1D chains and 2D lattices of SMA oscillators under gradient dynamic loading conditions.
- 5) Perform vibration experiments of a 1D chain and 2D lattice of SMA oscillators to validate the numerical and analytical results.

The technical approach will employ thermodynamics based constitutive modeling of SMAs, finite element analysis tools and structural non-linear dynamics of smart structures. This work will provide the basis for understanding the use of SMA elements in large scale space structures for the purpose of vibration isolation and damping. This report focuses on tasks 4 and 5. For information about the modeling effort of the dynamic response of SMAs refer to the publications section at the end of this report.

1.1 Shape Memory Alloys

SMAs are metals that are able to recover large amounts of inelastic strain (up to 8%), through a solid state phase transformation from an austenitic to a martensitic phase. The phase transformation can be induced by a change in stress or temperature. The stress-induced transformation is known as pseudoelasticity. Due to the hysteresis behavior associated with this transformation, SMAs show great potential for use in dynamic applications. Figure 1 shows an example of a complete pseudoelastic loading curve, with the corresponding hysteresis, along with a schematic of a partial transformation hysteresis. The area inside this curve represents dissipated energy, which would be the damped energy in a dynamic system.

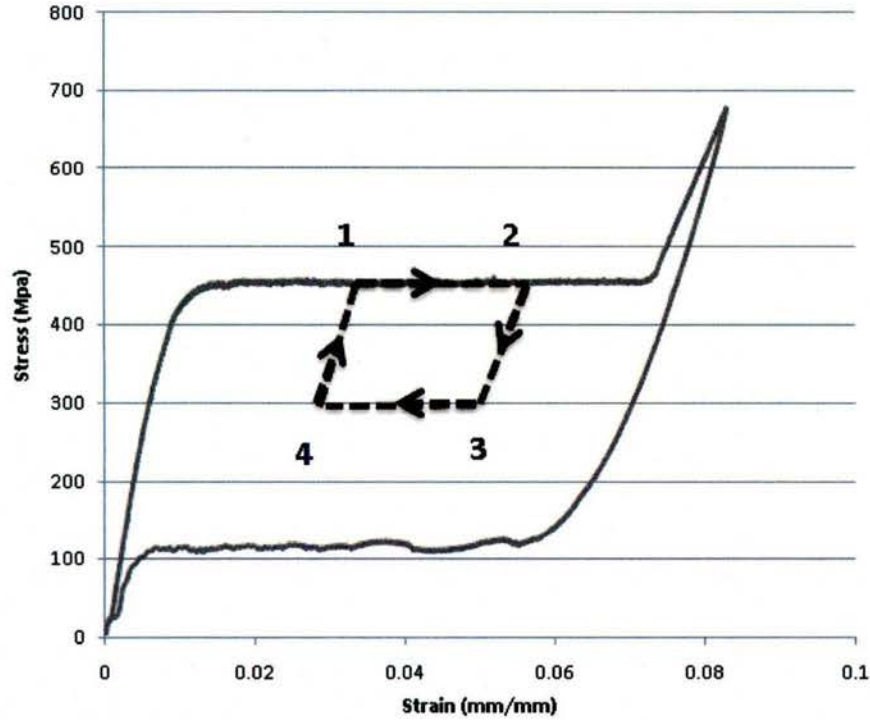


Figure 1 – Pseudoelastic response for SMA showing minor loop from points 1, 2, 3, and 4

In this report, three different sets experiments are presented and the results are discussed. These experiments were conducted over three years with the Air Force Office of Scientific Research to explore the response of the SMAs in dynamical systems. Specifically, the tests focused on the response in the frequency domain of the SMA's around the fundamental frequencies of each system in order to observe the non-linear jump. The first part of the experimental work involved studying a spring mass cart system. The second set of experiments utilized a shaker. Both sets of experiments included both a one degree of freedom and a two degree of freedom system. In all cases, Nitinol guide-BB-20 guidewire (55.8 wt% Ni 44.2 wt% Ti) from Memry Corporation was used.

2 Spring Mass Cart Experiments

2.1 Single Degree of Freedom

2.1.1 Experimental Setup

The one degree of freedom experimental setup consisted of two SMA springs, a 1.2 m Classic Dynamics System (track and mass cart), a Rotary Motion Sensor (PASCO CI-6538), and a Mechanical Oscillator/Driver (PASCO ME-8750). The power to drive the mechanical oscillator was provided by an 18VCD and 5A power supply (SE-9720A). A Vernier Sensor Data Acquisition Board (DAQ) was used to collect the measurement data from the Rotary Motion Sensor. Spring I was connected to the mass cart on one end and to the mechanical oscillator on the other end. The other spring, Spring II, was fixed at one end on the track and then connected to the mass cart on the other end. Figure 2 shows a picture of the experimental set up used for this single degree of freedom tests.

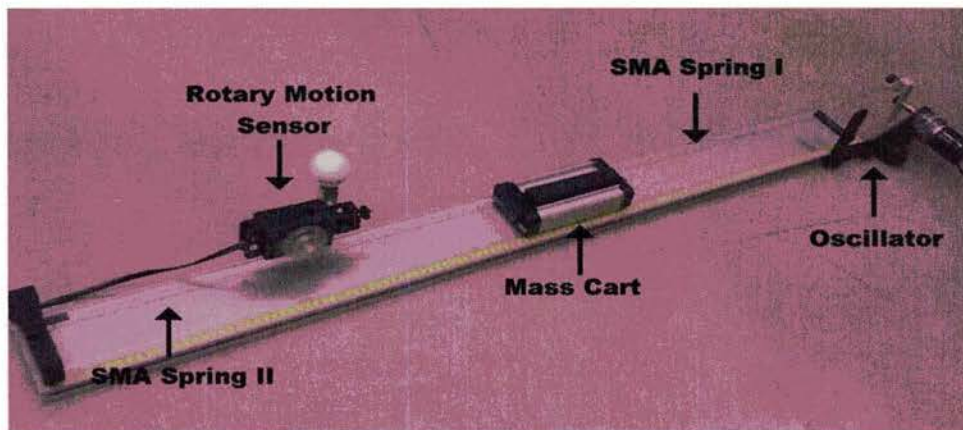


Figure 2 - Experimental setup of the mass and cart dynamical system showing the components and layout.

The string connecting Spring II and the mass cart was wrapped around the rotary motion's sensor pulley. The rotary motion sensor contained an internal wheel marked with 1440 equidistant points that were read by a laser thus allowing a system resolution of 0.25° or a linear resolution of 0.055 mm. The rotary motion sensor was connected to the DAQ system and the data was collected through LabView. The excitation frequency was varied by changing the power to the oscillator.

The SMA springs were prepared in lab using a threaded bar with two holes at each end. The guide-BB-20 SMA wire was wrapped around the threaded bar and kept in place with two screws going through the threaded bar holes. The threaded bar was then placed in an oven at 500°C for five minutes. After five minutes, the bar was taken out of the oven and water quenched for one minute, or until the bar was at ambient temperature. Steel springs were also used in this set-up to provide a linear response. These springs came prefabricated. Figure 3 shows a picture of the un-stretched springs used in these experiments.

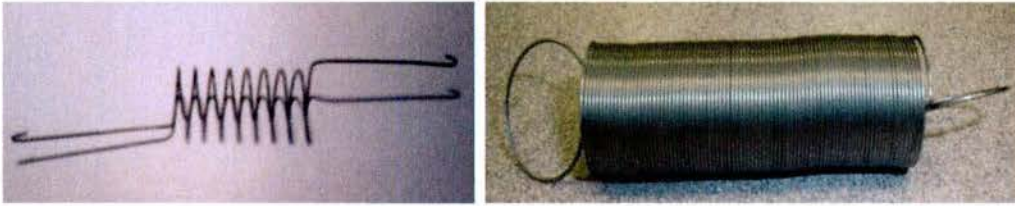


Figure 3 – Shape Memory Alloy spring (left) and steel spring (right)

2.1.2 Results

2.1.2.1 Force Displacement Behavior

To get the force displacement behavior of the springs, a uni-axial tension machine was used. The steep springs had to be cut as to not exceed the maximum displacement of the testing machine. Figure 4 shows the force-displacement curve for the steel spring, and Figure 5 shows the response of the SMA spring.

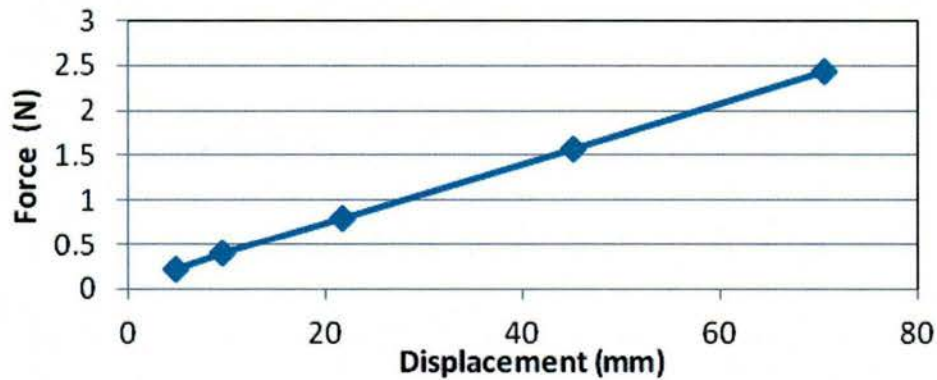


Figure 4 - Force vs. displacement for steel springs

The spring constant for the steel springs was obtained from the slope of the trend line in Figure 4 and was 3.4 N/m.

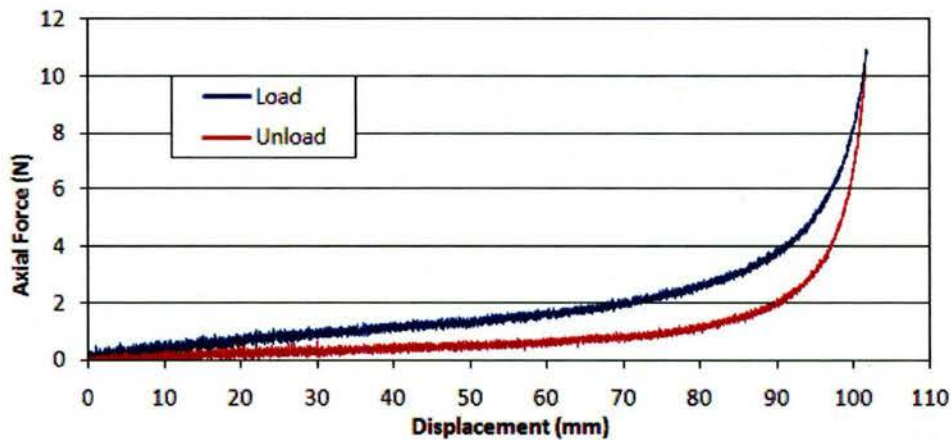


Figure 5 - Force vs. displacement for SMA spring

Likewise, the spring constant for the SMA spring was 3.0 N/m from linear part of the force displacement curve.

2.1.2.2 Free Response Analysis

The first tests conducted on the mass cart system were free response tests of the system in order to observe the damping behavior. The free response of both steel and SMA systems was performed using the same initial excitation amplitude of 12 cm. Once the initial amplitude is applied, the system is allowed to settle until no displacement is recorded. The free response for both cases is shown in Figure 6.

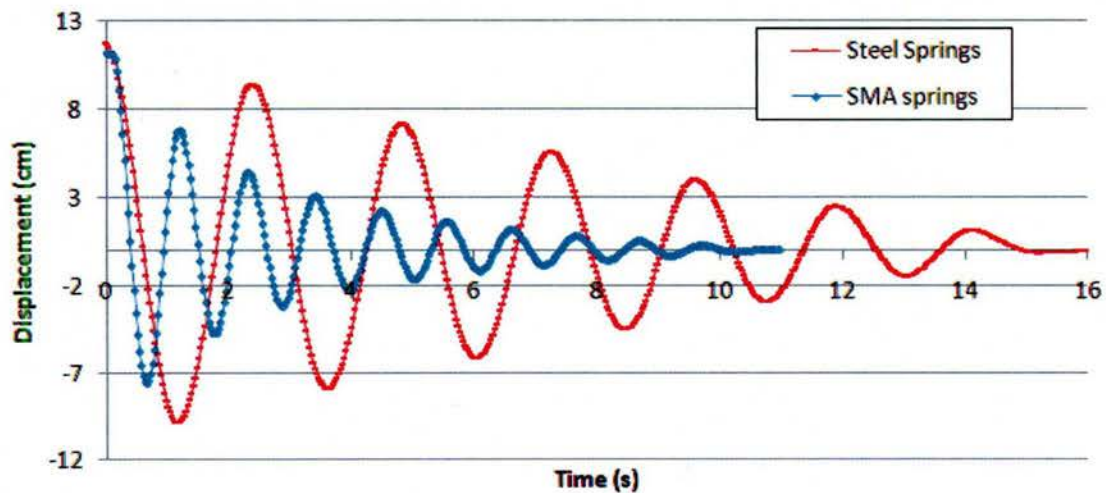


Figure 6 - Free response for steel and SMA springs

The damping coefficients of the steel and SMA springs were calculated with the log decrement method. This method provides an approximation which is appropriate for small damping ratios. *

$$\delta = \frac{1}{n} \ln \left(\frac{X_i}{X_n} \right) \quad (1)$$

Where δ is the logarithmic decrement, n is the number of peaks considered, X_i is the initial amplitude, and X_n is the amplitude of the peak, n periods away. Then, using the logarithmic decrement the damping ratio, ζ , can be calculated using Equation 2:

$$\zeta = \frac{1}{\sqrt{1 + \left(\frac{2\pi}{\delta} \right)^2}} \quad (2)$$

The damping ratio for the single degree of freedom system with steel springs was calculated to be 0.049, and that with SMA springs to be 0.067. The results from Figure 6 demonstrated that the SMA springs provide better damping than the steel springs. However, the damping of SMA's will be strain dependent, therefore the damping observed in Figure 6 will depend on the initial displacement of the test. The damping behavior of SMA's is associated with the amount of kinetic energy transformed into heat energy. This converted energy is equivalent to the area inside the hysteresis loop, which is strictly dependent on the amplitude of the strain.† Thus, the forced response needed to be analyzed in order to determine the energy dissipation in terms of strain amplitude.

2.1.2.3 Dwell Frequency Test Results Forced Response

Single frequency dwell tests were run through the range of the natural frequency of the system. The tests included a progression from frequencies below resonance to frequencies past resonance and a subsequent regression of frequencies from above resonance to frequencies below resonance. The behavior expected from the steel springs was an exponential increase in amplitude as the frequency approached the natural frequency. The amplitude was expected to reach a maximum at the natural frequency and then decreased exponentially again. As shown in Figure 7 and Figure 8, the tests were run with input frequencies ranging from 0.25 Hz to 1.2 Hz. Figure 7 shows the response of the steel spring.

* Gutenbrunner G., Savov K., & Wenzel H., Sensitivity Studies on Damping Estimation, Second International Conference on Experimental Vibration Analysis for Civil Engineering Structures (EVACES), Porto, Portugal (2007)

† Lammering, Rolf, and Schmidt, I., "Experimental Investigations on the Damping Capacity of NiTi Components." Smart Materials and Structures 10 (2001): 853-59.

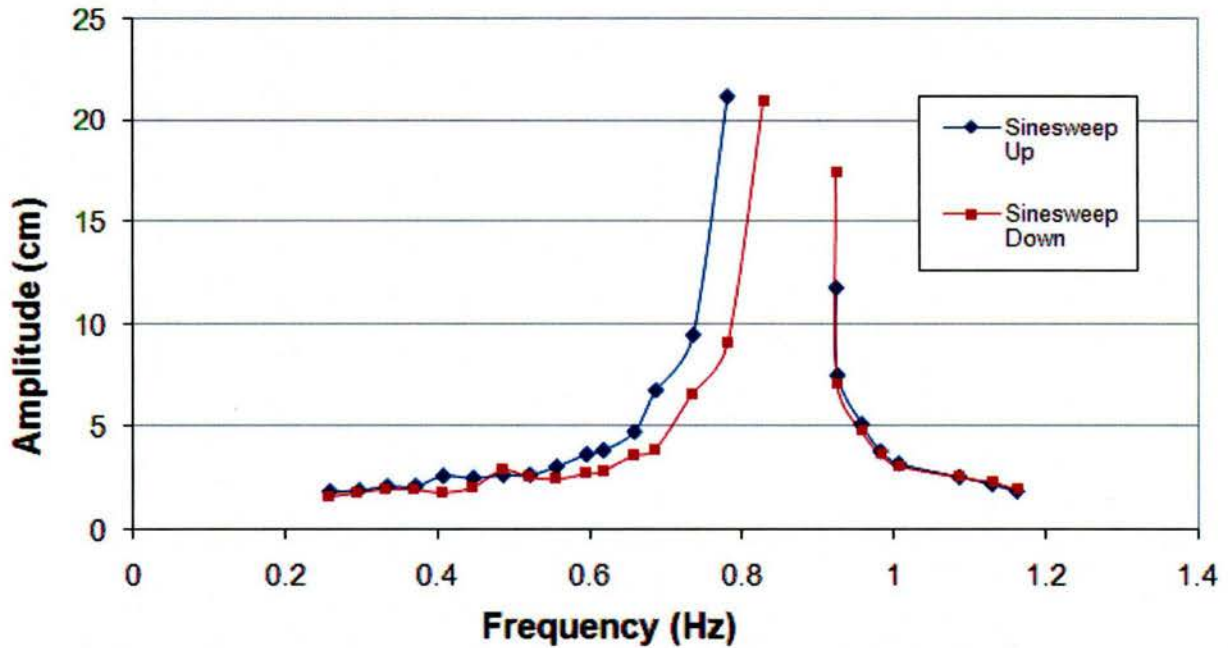


Figure 7 - Frequency response of steel spring system

Since the steel spring had very little damping, the displacement of the mass cart increased exponentially as the natural frequency was approached, between 0.83 Hz and 0.93 Hz. Amplitudes from 0.83 Hz to 0.93 Hz were not recorded due to the large magnitude of the displacement (over 40 cm). In the range of frequencies above the natural frequency, from 0.93 Hz to 1.2 Hz, the displacement showed an exponential decrease in the amplitude from 17.5 cm to 2 cm.

After the steel spring tests were completed, the SMA springs were tested. Figure 8 shows the response of the SMA spring system. Like before the frequencies were varied from 0.25 Hz to 1.2 Hz. The initial elongation was 120% for these tests.

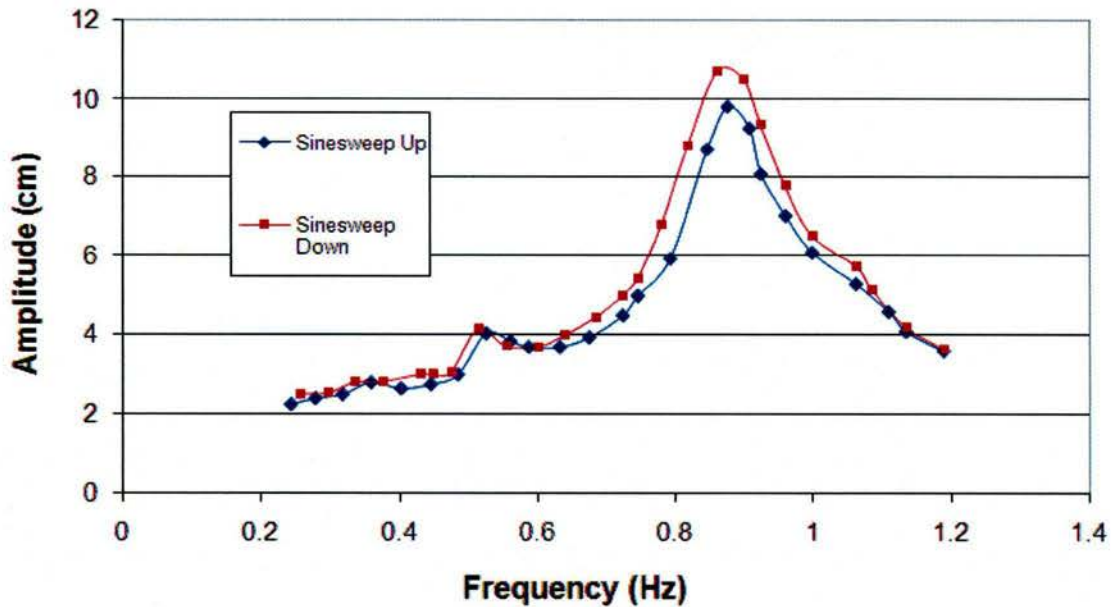


Figure 8 - Frequency response with SMA springs

The SMA springs exhibited similar behavior to the steel springs, with an exponential increase in the cart's displacement amplitude between 0.6 Hz and 0.9 Hz. At frequencies greater than 0.9 Hz the displacement magnitude decreases exponentially. When comparing the magnitudes of the displacements shown in Figure 7 and Figure 8, it can be concluded that the SMA springs exhibit much more damping than the steel springs. The SMA springs appear to be simply a linear system with increased damping, as the decrease in magnitude is the result of adding linear damping to a linear spring-mass system.

The linear type response observed in the experiments described in the above sections was not expected by the SMA springs. A discontinuous jump in the dynamic response was to be expected near the resonance frequency, rather than simply a damped system. In the next series of tests, the springs were at higher initial extension length (460%, rather than the 120% used above). Again, the same excitation was used, with taking incremental steps in frequencies from below resonance to above resonance. In this case, the initial frequency was set to 0.44 Hz and was increased to 1.72Hz by steps of 0.04Hz. The results are shown in Figure 9.

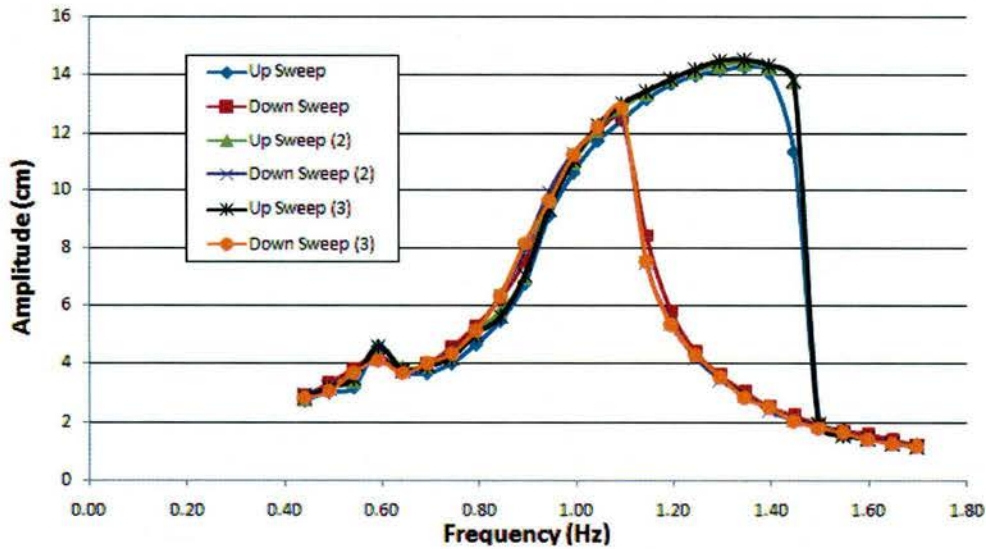


Figure 9 - Frequency response for SMA springs

The results shown in Figure 9 highlight the repeatability of this behavior. All three upsweep tests showed large jumps around excitation frequencies of 1.5 Hz. To further illustrate this behavior a plot of angular velocity vs. position was made and is shown in Figure 10.

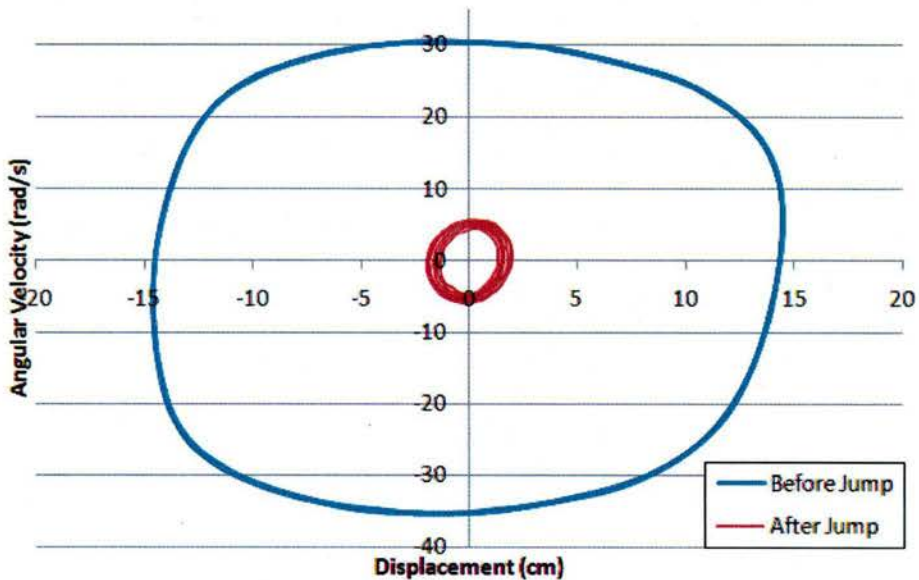


Figure 10 - Angular velocity vs. displacement for SMA springs

The angular velocity magnitude drastically decreases from approximately 30 rad/s to 5 rad/s going from 1.4 Hz to 1.51 Hz as shown in Figure 10. The jump demonstrates the difference between the linear response of the steel springs and SMA springs that are pre-stretched enough for transformation to occur. The mass cart system results illustrate how the characteristic jump is an important aspect of the SMA's dynamic response.

2.1.3 Discussion

The single degree of freedom experiments with the classical spring mass-cart system revealed three important results:

- The SMA springs provide an increase in free response damping ratio over linear steel springs.
- The SMA springs exhibit a unique jump in amplitude during a sine sweep if sufficient pre-stretch is applied.

These results were significant, but investigation of more complex systems was needed in order to gain a deeper understanding of the complexities of using SMAs in dynamic systems.

2.2 Two Degree of Freedom Mass Spring Experiment

2.2.1 Experimental Setup

The two degree of freedom experiments were conducted on the same set up as before, but with two mass carts. The SMA springs were all manufactured in the same fashion as described in Section 2.1.1. The DAQ system used could only capture displacements of one mass cart for each experiment. To get a complete data set, the rotary motion sensor was used on the first mass cart (mass cart I) and then used on the second mass cart (mass cart II) in successive experiments. A picture of the setup, Figure 11, shows how the rotary motion sensor was connected to read the amplitude of mass cart II.

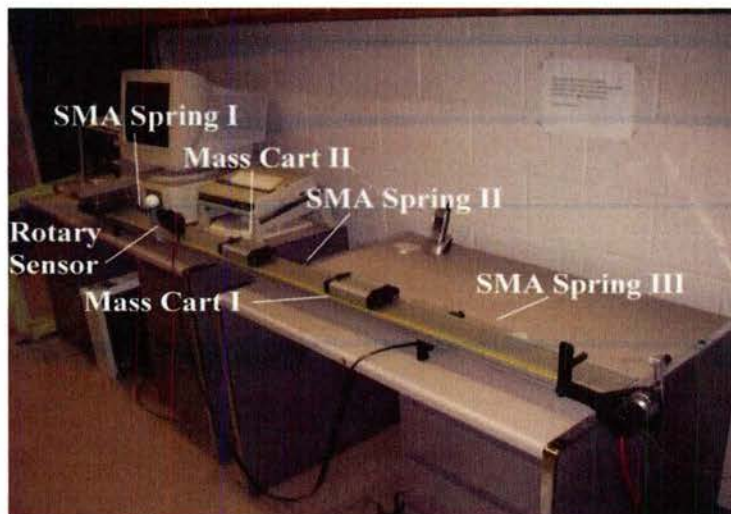


Figure 11 – Two degree of freedom mass cart system

2.2.2 Testing

Using the oscillator, the mass carts were put through a frequency sweep to observe both eigen frequencies. Because of a limited track length, the maximum pre-stretch applied to the springs was two times their original length (200%). The sweep was started at 0.3 Hz and gradually increased at 0.0057 Hz/sec. The results are shown in Figure 12 for mass cart I and Figure 13 for mass cart II.

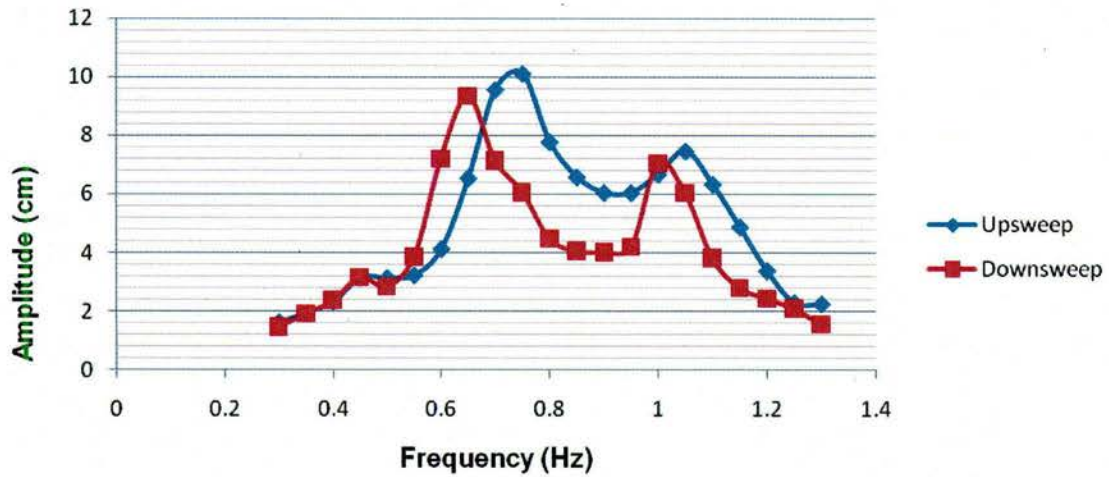


Figure 12 – Mass cart I amplitude vs. frequency sine sweep

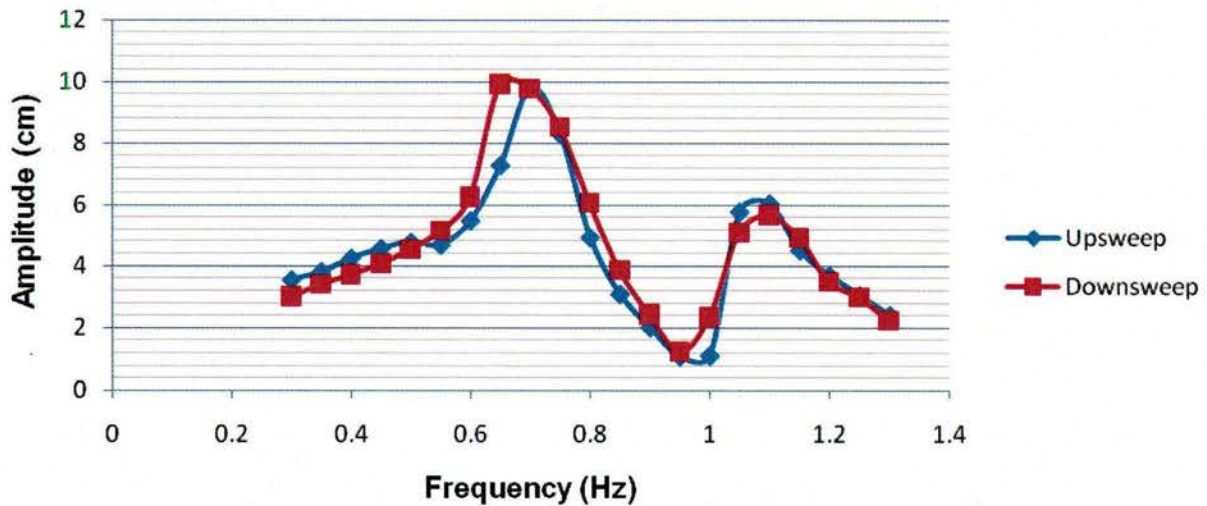


Figure 13– Mass cart II amplitude vs. frequency sine sweep

During upsweep, the first eigen frequency of 0.7 Hertz corresponded to in-phase vibration when both mass carts moved together. The second eigen frequency of 1.05 Hertz was out-of-phase vibration when both mass carts were completely out of phase from each other.

Despite multiple tests, the SMA springs broke on most of the experiment. When a spring broke, it was replaced and the test was resumed at the frequency at which it broke, since this was small incremental steps through the frequency range, the breaking of springs will not significantly alter the results.

2.2.3 Discussion

The two degree of freedom mass cart system experiments on SMA springs furthered the work done by the single degree of freedom experiments in three ways. First, the dwell test results show that jumps occur at both eigen frequencies corresponding to in-phase and out-of-phase vibration. Second when the jump occurs, the change in amplitude is instantaneous.

3 Shaker Experiments

The second set of experiments was conducted on a shaker table. A mass was suspended with SMA and steel wires from a frame rigidly attached to the shaker. These experiments examined the behavior of the SMAs in a different, geometry, and would more representative of the proposed large sparse aperture array application. The shaker experiments were broken into two sections, the single degree of freedom system and the two degree of freedom system.

3.1 Single Degree of Freedom Vibration Experiment

3.1.1 Experimental Setup

As an extension to the research done on the one degree of freedom mass cart and spring system, tests were performed on a one degree of freedom vibration setup with a shaker table as shown in Figure 14. The setup involved a single mass suspended vertically along two metal rails by two SMA wires. The mass was allowed to slide along the two metal rails with negligible friction due to ball bearings. The motion of the mass was recorded by a uni-axial accelerometer. Three additional uni-axial accelerometers were placed on the setup to provide feedback to the shaker control software. The top and bottom SMA wires were set to a specific pre-strain. The pre-strain was determined geometrically and verified via a load cell on the top grip. Thermocouples were applied to both SMA wires.

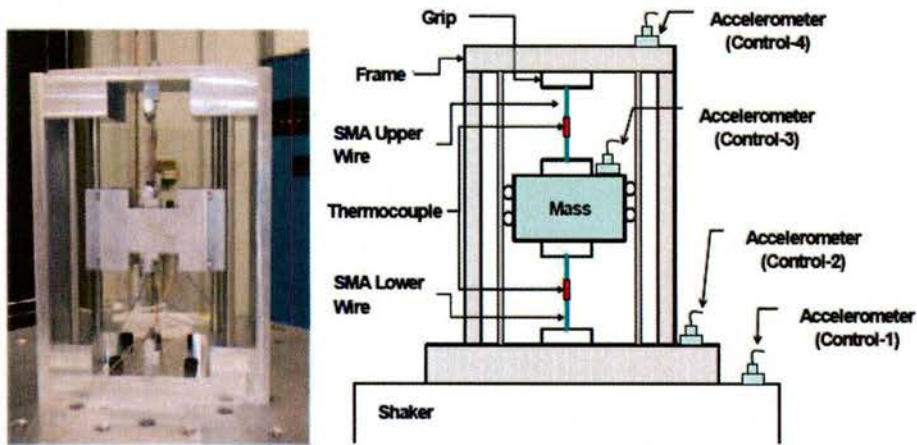


Figure 14– Setup for one degree of freedom vibration experiment

The SMA wires were the same wires used for the SMA springs. This was the same material used to make the springs.. In order to stabilize the transformation response, training of 30 cycles were performed on all wires used in the experiments. The training process involved stress induced transformation under isothermal conditions. The wires were loaded to 800 MPa which corresponded to 9% strain and complete transformation to

Martensite. Then, the SMA was unloaded and allowed to undergo reverse transformation back to austenite. Since the wires were pseudo-elastic at room temperature, no heating or cooling of the wires was used.

3.1.2 Testing

The first part of testing involved training and characterization of the SMA wire. The characterization was done in a uni-axial load frame. The next part of the testing was focused on the vibration response of the SMA wires on the shaker. The experiments for the vibration system involved characterizing the difference in the sine sweep response and dwell test response at resonance. The sine sweep test involved a constant magnitude of acceleration applied to the system by the shaker table over a range of frequencies. This form of testing reveals the natural frequency of the system and any non-linearities that are present. Such non-linear responses from the SMA wires appear as a jump in the mass's acceleration in a similar fashion to the amplitude jump from the mass cart experiments. The dwell tests were used to study the output acceleration at specific frequencies near resonance. By holding the input magnitude acceleration constant at a non-changing frequency, it was possible to see if the SMAs exhibited a chaotic response during transformation. Thus, by comparing the results from the sine sweep and dwell tests, it was possible to observe non-linearity in the dynamic response and determine if the SMAs have a chaotic response at resonance.

3.1.2.1 Material characterization

The experimental set up is built with the same NiTi SMA wires that were trained with 30 loading/unloading cycles at room temperature shown in Figure 15. The main purpose of training the wires was to stabilize the hysteresis behavior. After the training was completed, three loading/unloading cycles at temperatures of 25, 30, and 40°C were performed, shown in Figure 15.

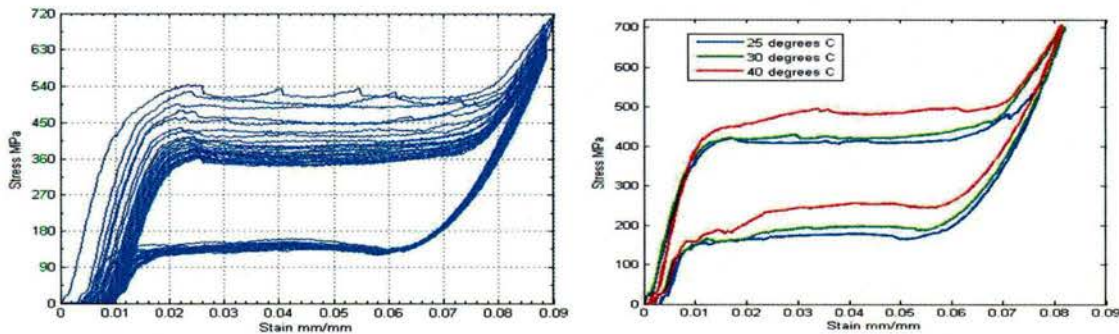


Figure 15 – Stress vs. strain curves for 30 loading/ unloading cycles at room temperature (left) and three different ambient temperatures(right)

3.1.2.2 Sine Sweep Vibration Tests

Sine-sweep vibration tests frequency range went from 32Hz to 256Hz at a rate of 1.244 Hz/sec. The input acceleration amplitude was 1g. The SMA wires were strained to 4% prior to testing. The 1g up and down sweep tests results are shown in Figure 16.

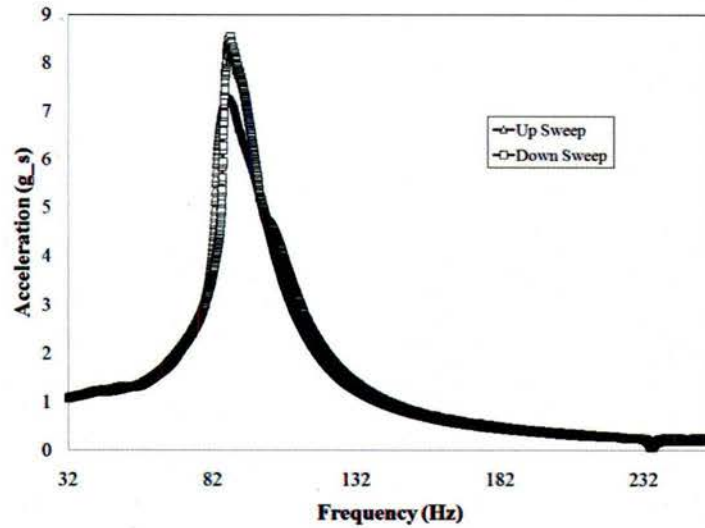
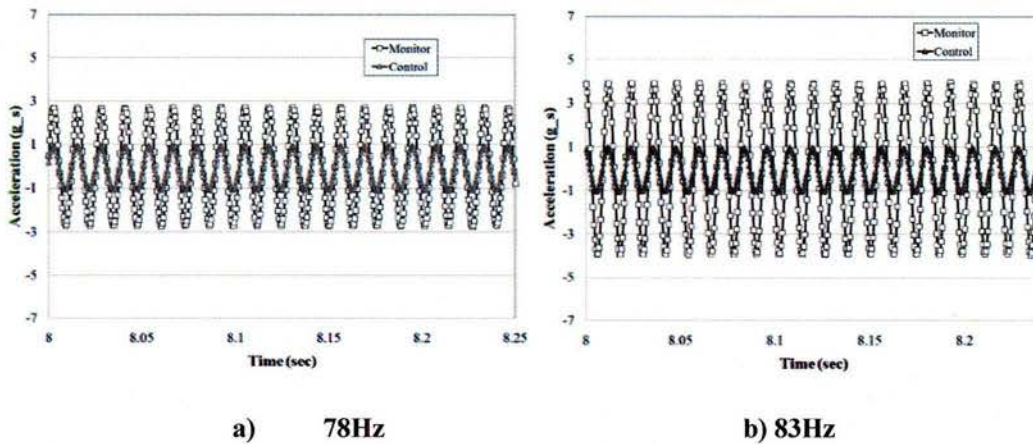


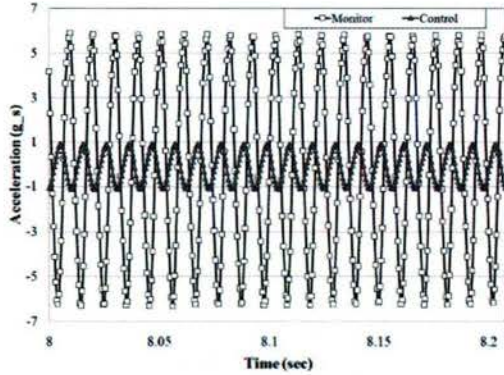
Figure 16 – Frequency response for up and down sweep sine sweeps with input acceleration of 1g

The peak occurred at 83Hz, for the up sweep, and 84Hz, for the down sweep. This response is similar to what was to be expected for a linear system. It is assumed that a jump similar to what was shown in Figure 9 would occur at the frequency of these peaks.

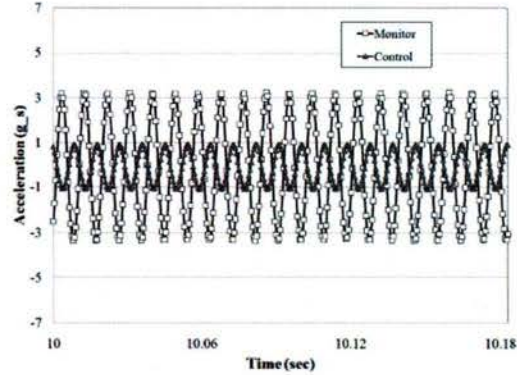
3.1.2.3 Single Frequency Dwell Tests

To further investigate if the jump behavior could be observed dwell tests were performed. Four different dwell tests were performed, at 78, 83, 96 and 109 Hz. These frequencies were chosen because to see the behavior below and above resonance. The dwell results at the natural frequency, 83Hz, were compared with data from the three other frequencies. Figure 17 shows 20 periods of results for all dwell frequencies with control and monitor acceleration data. Control refers to the acceleration of the frame. Monitor refers to the acceleration of the suspended mass.





c) 96Hz



d) 109Hz

Figure 17– Single frequency dwell results for a) 78 Hz b) 83 Hz c) 96 Hz, and d) 109 Hz for 20 periods

In Figure 19b, the expected jump frequency, constant amplitude was kept for the duration of the test. However the amplitude magnitude at the jump frequency, 83Hz, deviated from the amplitude observed during sine sweep testing while the other frequencies matched amplitudes for the resonant curve and single frequency dwell. Table 1 compares the amplitudes for each frequency from the resonant curve and single frequency dwell tests.

Table 1 – Amplitudes tabulated for tested dwell frequencies along with their corresponding resonant curve amplitude value

Frequency	Resonant Curve (g's)	Single Frequency (g's)	Difference (%)
78 Hz	2.9	2.7	6.9
83 Hz	5.5	3.9	29.1
96 Hz	5.8	5.8	0.0
109 Hz	3.0	3.2	6.7

The deviation of the jump frequency was around four times greater than that of the 78Hz and 109Hz values.

3.1.3 Discussion

The results found contribute to two findings. First, it was hypothesized that the output of a frequency in the jump could be erratic, changing amplitudes with time. However, this was not observed and the output of the device when subjected to a frequency at the jump was sinusoidal and kept a constant amplitude. Secondly, it was found that the amplitude for the jump frequency of the dwell tests deviated from the amplitude observed at the same frequency during sine sweep tests. This could be a result of the nonlinear behavior shown in Figure 9. Since the shaker brought the frequency

up to the dwell frequency, the behavior would be similar to the upswEEP behavior and the magnitude should be greater than at the natural frequency.

3.2 Two Degree of Freedom Experiment

3.2.1 Experimental Setup

The setup used for the two degrees of freedom vibration tests involved a hoop with central mass suspended by tensioned SMA wires. The first part of the design was the base structure. Four bolts attached the base plate to the shaker, Deeritron VP-70 Shaker Table, as shown in Figure 18. The mass hoop was attached to the base with three bolts (denoted as Bolt in Figure 18); one in the bottom of the hoop, and one on each side at half of the height of the hoop. The suspended mass was a hollowed out cube. A uni-axial accelerometer was placed inside the suspended mass with different orientations depending on the test. The mass's total weight is 0.71 kg.

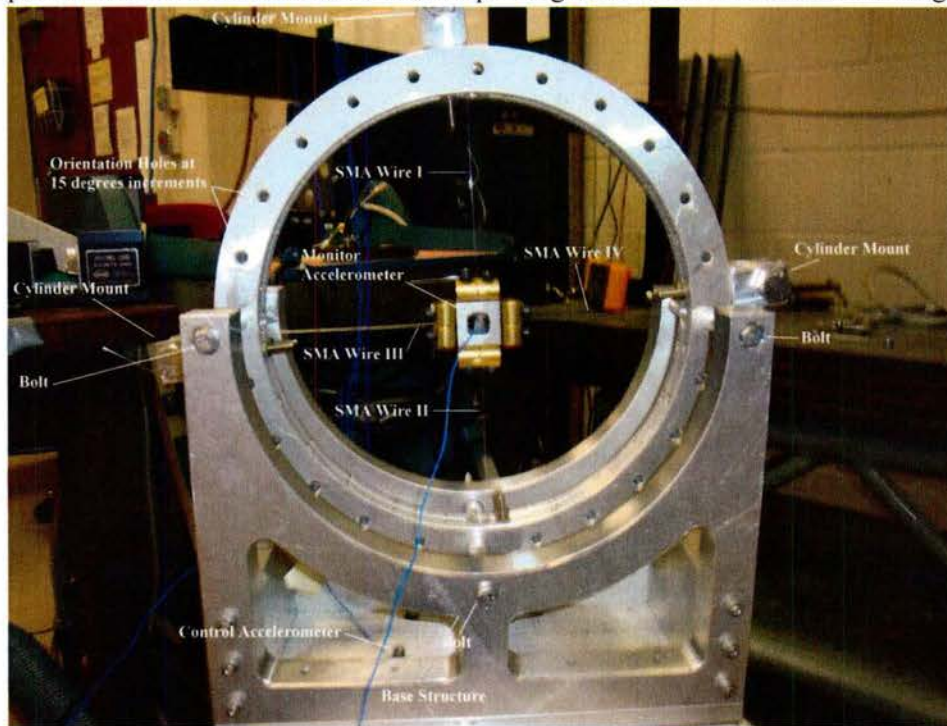


Figure 18 – Setup for two degrees of freedom vibration experiment

Along the sides of the hoop are four cylinder mounts that set the pre-strain on each of the SMA wires individually as shown in Figure 18. The SMA wires were attached to the hoop by a cylinder mount, shown in Figure 19.

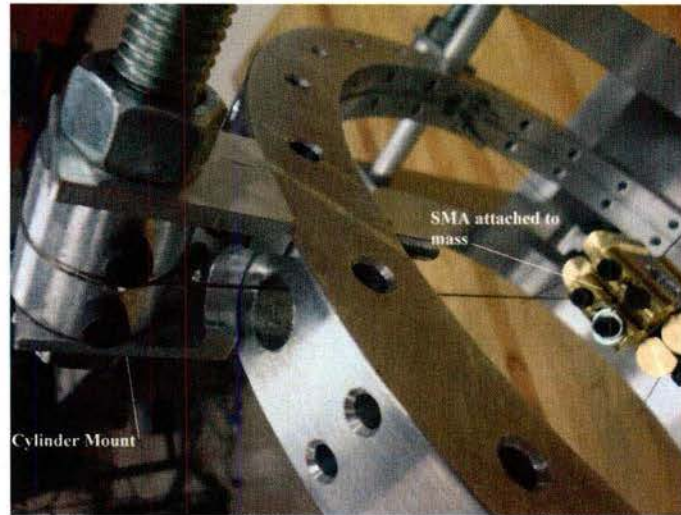


Figure 19 – Cylinder mounts for SMA wires

The cylinders were rotated to generate the required initial strain in the wire which was monitored by placing an extensometer on the wire. After the specific strain was applied, the cylinders were firmly constrained against the hoop.

The SMA wires were trained with a peak stress level of 800 MPa, corresponding to a strain of 9%, as described in section 3.1.2.1. The results of the training are shown in Figure 20.

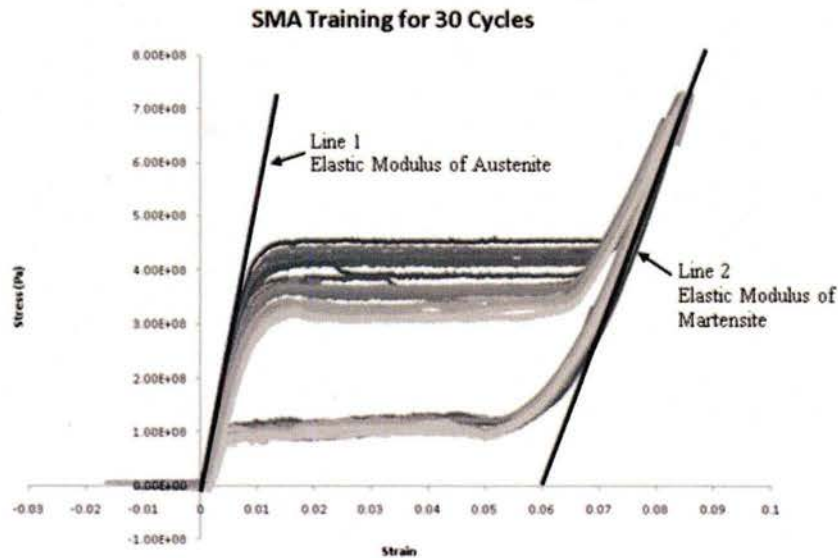


Figure 20 – Results for 30 cycles of training for SMA wires

Two tangent lines were drawn on the training curves of the last training cycle, to obtain an elastic modulus for each phase. The maximum transformation strain achieved by the SMA is 6% as measured by the x-axis intercept of the second tangent line. Thus, in order to achieve transformation during testing, a strain value of 3% was determined to be the initial strain for the vibration testing.

3.2.1.1 Pre-strain of the SMA Wires

To get the correct amount of initial strain, a jig was used to hold the suspended mass in place while the strain was applied. An extensometer was attached to the wire, and the strain was adjusted to the desired value using the cylinder mounts. Care was taken to ensure that the extensometer weight was offset by an external source (the circular frame here) such that the weight of the extensometer did not stretch the wire. The setup used to set the initial strain is shown in Figure 21.

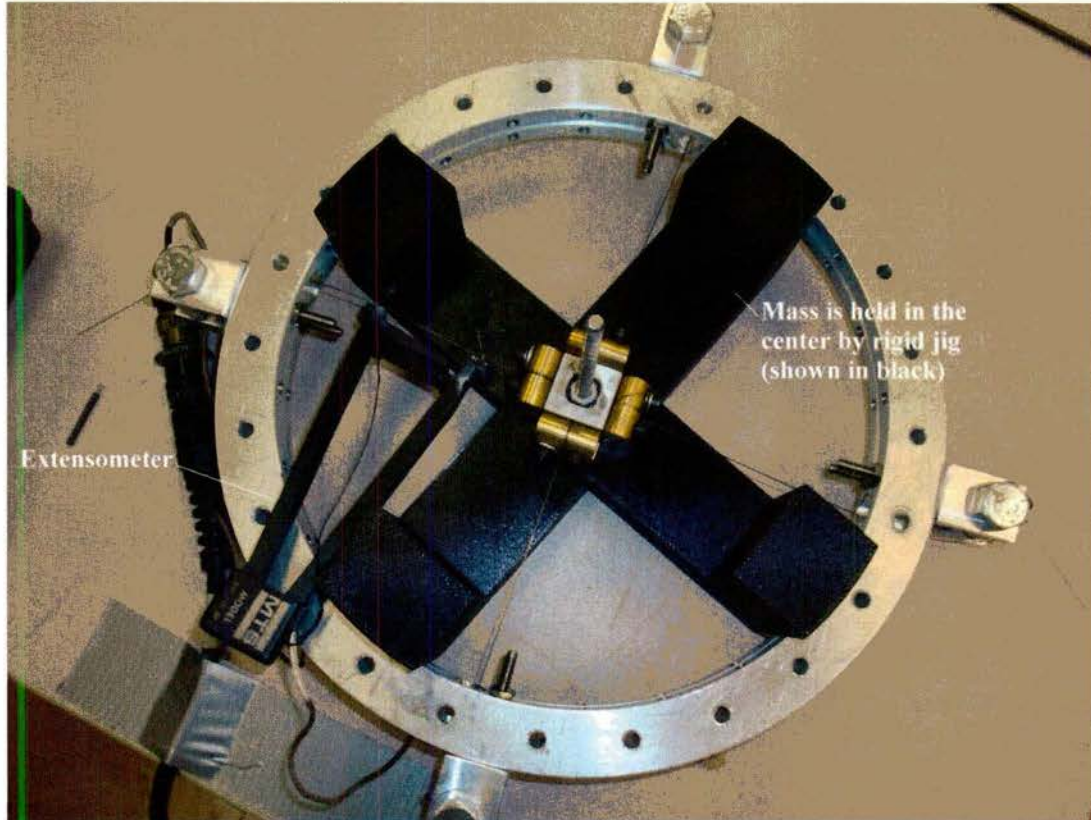


Figure 21 – Strain measurements for the two degrees of freedom experiment

3.2.2 Testing

3.2.2.1 Sine Sweep Tests for Elastic Modulus

Similar to the one degree of freedom vibration tests, several sine sweep tests were performed. The first test was conducted on wires that were completely in the martensite phase, which was controlled via pre-straining. Using the relationship between the resonant frequency and the elastic modulus, it was possible to compare the modulus values determined from the sine sweep experiments with the slope of the tangent lines found during training. For this analysis, the elastic modulus of the SMA was related to the natural frequency with an elastic material approximation given by Equation 3.

$$\text{Elastic Modulus} = \frac{m * L * (\omega_n)^2}{A} \quad (3)$$

Where m is the mass suspended by the pre-strained wires, L is the length of the wire, ω_n is the natural frequency, and A is the cross-sectional area of the wires.

The natural frequency from an SMA at 10 % pre-strain, or fully martensite, was used to calculate the elastic modulus of martensite. The modulus was compared to the modulus found during training. The result of the shaker experiment for the fully martensitic wires is shown in Figure 22.

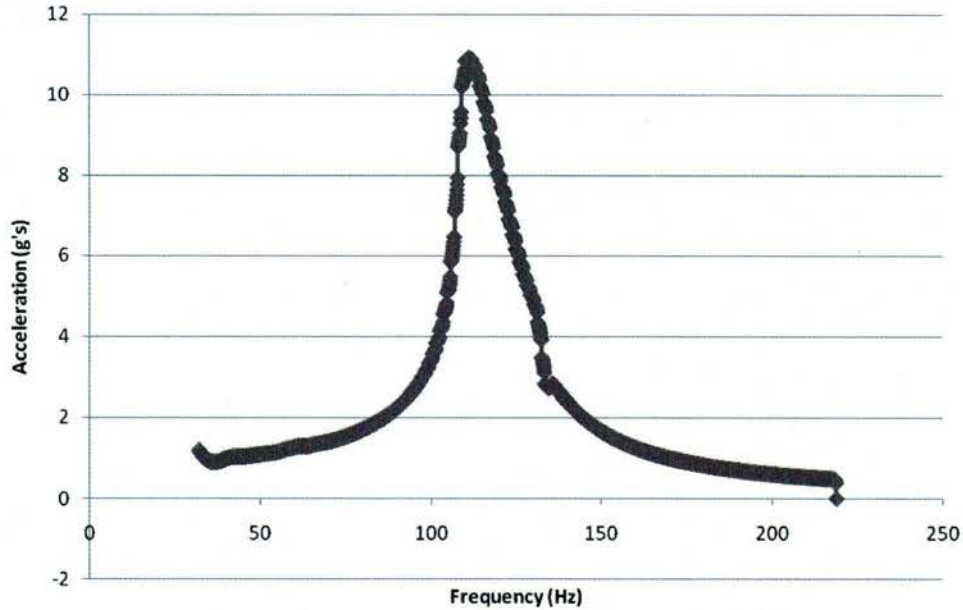


Figure 22 – Sine sweep results for SMA with 1 g excitation for fully martensite test

With a natural frequency of 106 Hz in the martensite phase, the elastic modulus according to Equation 3 was 30.6 GPa. The elastic modulus determined via training was 32.5 GPa. This shows that the sine sweep results for elastic modulus values closely match the results obtained from the training.

3.2.2.2 Comparison with Steel

After the fully martensitic test was performed, the response of the partially transformed SMA wires was compared with that of the steel wires. The objective was to compare the damping ability of both materials. The SMA had an initial strain of 3% to ensure transformation would take place and would maximize the amount of damping.

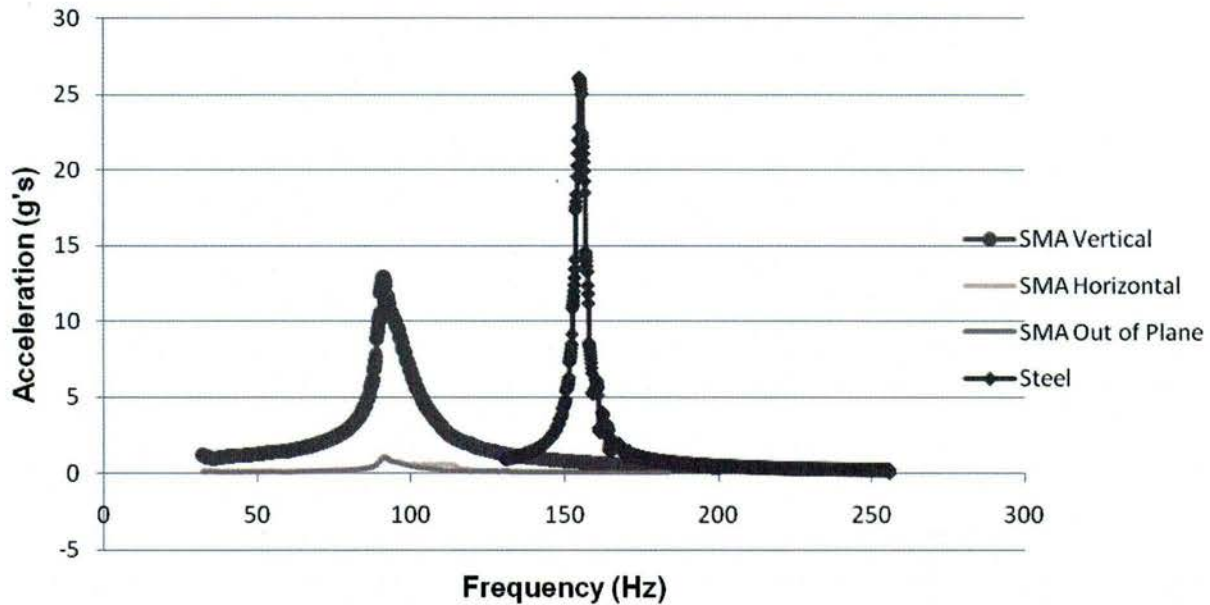


Figure 23 – Comparison of SMA and steel with 1 g excitation

The SMA response has both a lower peak and a much wider bandwidth which indicates improved damping over the steel.

3.2.2.3 Damping Ratio

To quantitatively compare the damping behavior, estimations of the damping ratios were computed. The half power rule was used in to get an approximation of the damping ratio. This method is an approximation for a linear spring-mass-damper system based on the fact that in these systems the bandwidth of the response amplitude is proportional to the damping ratio.[‡] By taking the peak amplitude and dividing by $\sqrt{2}$, it was possible to get the half power amplitude needed to calculate the damping ratio from the bandwidth of the amplitude vs. frequency plot. The equation for the damping ratio from the half power rule is given as:

$$\zeta = \frac{\omega_1 - \omega_2}{\omega_n} \quad (4)$$

where ω_1 and ω_2 are the radial velocities at the half power amplitude found from dividing the primary peak amplitude by a factor of $\sqrt{2}$, and ω_n is the natural frequency of the system, which corresponds to the primary peak amplitude. The SMA wires pre-strained to 3% in Figure 23 had a damping ratio of 0.078. From the experiments, the highest damping ratio for the SMA was observed when the SMA was pre-strained to 10%, fully martensite. For the SMA wires in the fully martensitic phase, the damping ratio was equal to 0.117 as shown in Figure 22. This is a dramatic improvement over the steel wires with a damping ratio of 0.017. Both graphs are superimposed to show this difference. This result is shown in Figure 23.

[‡] Gutenbrunner G., Savov K., & Wenzel H., Sensitivity Studies on Damping Estimation, Second International Conference on Experimental Vibration Analysis for Civil Engineering Structures (EVACES), Porto, Portugal (2007)

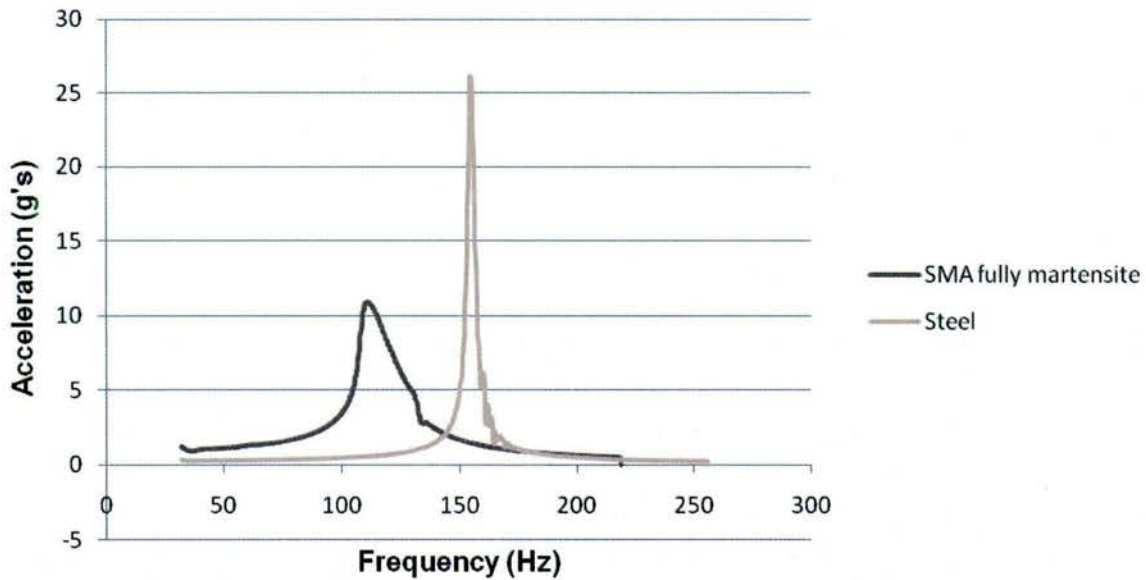


Figure 24 – Comparison of martensitic SMA with steel in sine sweep

3.2.2.4 Dwell Test Comparison with Sine Sweep Results

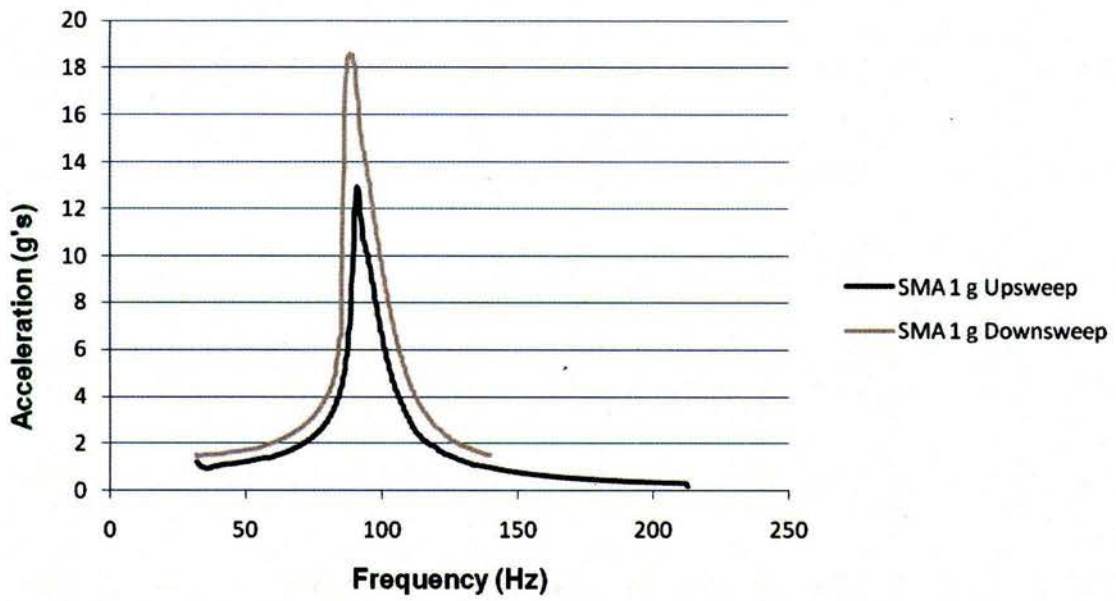
Dwell tests were performed at frequencies near the up sweep resonant frequency of 90 Hz for the case of 3% initial strain. The dwell tests were performed at 85 Hz, 90 Hz, 95 Hz, and 100 Hz. These tests showed no change in acceleration over time which indicates there is no chaos in the system. Instead, the output acceleration from the dwell tests once again differed from the acceleration observed in the sine sweeps before and at the jump frequency of 90 Hz. These differences were tabulated, and the results are shown in Table 2.

Table 2 – Difference in acceleration between dwell tests and sine sweeps

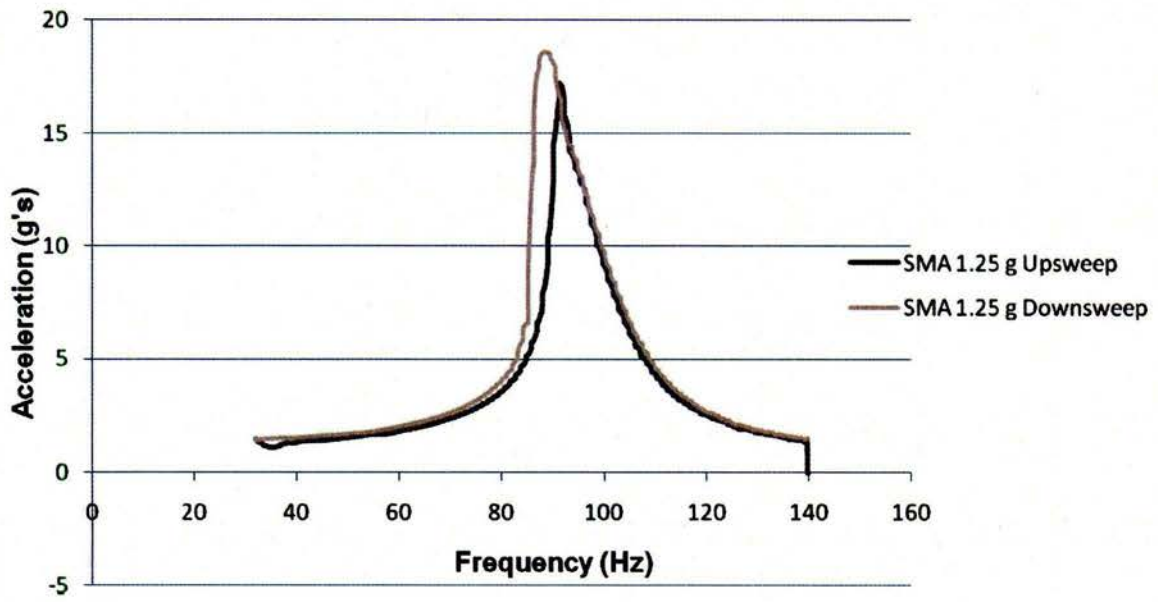
Frequency	Resonant Curve (g's)	Single Frequency (g's)	Difference (%)
85 Hz	4.4	5.6	21.4
83 Hz	12.0	14.8	18.9
96 Hz	10.0	9.6	4.2
109 Hz	6.7	6.1	9.8

3.2.2.5 Phase Transformation and Non-linear Response

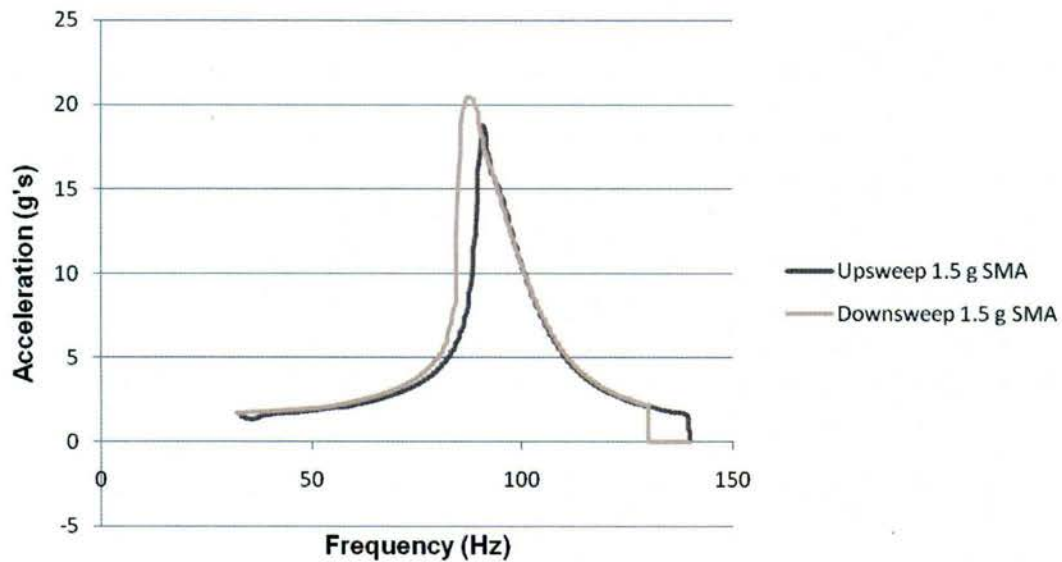
To further investigate the non-linear behavior of the SMA wires, the input acceleration magnitude was varied. Three different tests were conducted with input acceleration magnitudes of 1g, 1.25g and 1.5g. The graphs of the upsweeps and down sweeps are shown in Figure 25. The deviation is a result of the hysteresis and exploits the non-linearity of SMA's in dynamics systems.



a)



b)



c)

Figure 25 – Comparison of up and down sweep for SMA wires with acceleration input magnitudes of a) 1 g, b) 1.25 and c) 1.5 g

As the input acceleration is increased, the down sweep resonant frequency shifts away from the resonant frequency from the upsweep. The larger magnitude increases the effects of the hysteresis and the nonlinearity become more prominent. The differences were calculated and are shown in Table 3.

Table 3 – Comparison of Upsweep and Down sweep Natural Frequencies

Experiment	1 g Input	1.25 g Input	1.5 g Input
Up sweep (Hz)	90.9	91.3	90.4
Down sweep (Hz)	88.5	88.5	87.5
Difference (%)	2.4%	3.1	3.3

4 Publications

4.1 Text book

Lagoudas, D.C, Shape Memory Alloys: Modeling and Engineering Applications, Springer-Verlag 2008.

4.2 Refereed Journal Articles

Kalmar-Nagy, T. and Shekhawat, A., “Nonlinear Dynamics of Oscillators with Bilinear Hysteresis and Sinusoidal Excitation”, *Physica D Nonlinear Phenomena* (2009).

Machado, L., Lagoudas, D., and Savi, M., 2009, "Lyapunov Exponents Estimation for Hysteretic," *International Journal of Solids and Structures*, 46, pp. 1269-1286.

4.3 *Conference Proceedings and Papers*

Machado, L.G. and Lagoudas, D.C., "Nonlinear dynamics of a SMA passive vibration isolation device," Proceedings of SPIE Vol. 6169, SPIE, San Diego, CA, February 28-March 2, 2006.

Machado, L.G. and Lagoudas, D.C., "Nonlinear Dynamics and Chaos of a SMA Passive Vibration Isolation and Damping Device", Vol. 6525, SPIE 2007, San Diego, CA, March 18-22, 2007.

Machado, L.G. and Lagoudas, D.C., "Nonlinear dynamics of a SMA passive vibration isolation device," Proceedings of SPIE Vol. 6169, SPIE, San Diego, CA, February 28-March 2, 2006.

Machado, L.G. and Lagoudas, D.C., "Nonlinear Dynamics and Chaos of a SMA Passive Vibration Isolation and Damping Device", Vol. 6525, SPIE 2007, San Diego, CA, March 18-22, 2007.

Machado, L.G. and Lagoudas, D.C., "Numerical-Experimental Investigation of the Dynamics of a Shape Memory Alloy Passive Vibration Isolation and Damping Device", AIAA-SDM, Honolulu, HI, April 23-26, 2007.

Machado, L., Lagoudas, D.C., and Savi, M.A. "Estimation of Lyapunov Exponents for Chaotic Hysteretic Systems," SES Conference, College Station, TX, Oct. 21-24, 2007.

Kalmar-Nagy, T., Shekhawat, A., and Lagoudas, D.C. "Dynamic Response of Hysteretic Shape Memory Alloy Oscillators," SES Conference, College Station, TX, Oct. 21-24, 2007.